MJoSHT
Malaysian Journal of Science, Health & Technology
[mjosht.usim.edu.my]

USIM

Article

Facile Preparation of Gold Nanoparticles/Silica Composite Film Embedded in Anodized Aluminium Oxide-Glass Substrate

Mohamad Azani Abd Khadir Jalani[1], Juan Matmin[2], Siew Ling Lee[2], Syaza Azhari[3], Mohd Hayrie Mohd Hatta[4] and Nur Fatiha Ghazalli[5]

[1]*Kolej PERMATA Insan, Universiti Sains Islam Malaysia, Bandar Baru Nilai, 71800 Nilai, Negeri Sembilan, Malaysia.*

[2]*Department of Chemistry, Faculty of Science, Universiti Teknologi Malaysia, 81310 UTM Johor Bahru, Johor, Malaysia.*

[3]*Faculty of Science and Technology, Universiti Sains Islam Malaysia, Bandar Baru Nilai, 71800 Nilai, Negeri Sembilan, Malaysia.*

[4]*Centre for Research and Development, Asia Metropolitan University, 81750 Johor Bahru Johor, Malaysia.*

[5]*School of Dental Sciences, Health Campus, Universiti Sains Malaysia, Kubang Kerian 16150, Kota Bharu, Kelantan, Malaysia.*

Correspondence should be addressed to:

Mohamad Azani Abd Khadir Jalani; mazani@usim.edu.my

Article Info
Article history:
Received: 9 February 2024
Accepted: 4 April 2024
Published:5 April 2024

Academic Editor:
Mohd Hafiz Abu Hassan

Malaysian Journal of Science, Health & Technology

MJoSHT2024, Volume 10, Issue No. 1
eISSN: 2601-0003

https://doi.org/10.33102/mjosht.v10i1.402

Copyright © 2024 Mohamad Azani Abd Khadir Jalani et al.

This is an open access article distributed under the Creative Commons Attribution 4.0 International License, which permits unrestricted use, distribution, and reproduction in any medium, provided the original work is properly cited.

Abstract*— Thin film based on gold nanoparticles or AuNPs is typically used as catalyst in the industrial processes due to their high stability and good reusability. In this work, a thin AuNPs-silica composite film was fabricated firstly from sol-gel method by mixing gold(I) pyrazolate complex to medium comprised of ethanol, deionized water, and hydrochloric acid, followed by addition of tetrabutyl orthosilicate as silica source. Next, 70 μL of the sol-gel solution were spin-coated on several type of substrates such as glass, anodized aluminium oxide or AAO, and combination of both to yield gold complex/silica composite thin film. It was found that gold complex/silica composite film fabricated on combination of both AAO-glass substrate gave the best quality based on its surface thickness, layer uniformity and film brittleness. Later, the thin film was selected and subjected to thermal hydrogen reduction at 210 °C for 2 hours to facilitate the formation of gold nanoparticles to give AuNPs/silica_AAO-glass film. Before the heat treatment, the light-brownish colour of the original gold complex/silica_AAO-glass film in daylight will appear as a pinkish red film under UV light, suggesting the interaction between gold atoms as supported by its luminescence spectrum at 692 nm. Upon heat treatment, the resulting AuNPs/silica_AAO-glass film gave a deep-red colour indicating the successful formation of AuNPs. The presence of AuNPs in the film was further confirmed based on its absorption peak at 545 nm, X-ray diffraction pattern at 2θ = 38.20° for d_{111} plane in wide-angle region, transmission electron microscopy images showing a small and sphere shape particles as well as its elemental composition in energy dispersive X-ray analysis. Moreover, scanning electron microscope images of AuNPs/silica_AAO-glass film also suggested that the AAO pores is fully filled with the composite and is in accordance with its surface roughness study via atomic force microscopy analysis.

***Keywords*— Anodized aluminium oxide; glass; gold nanoparticles; thin film**

I. INTRODUCTION

Nanocomposites can be defined as the materials made up of two or more unsimilar components, such as organic/ inorganic materials with one of its respective phases is in nano-sized dimension [1]. For example, silica nanomaterials with small pore size have gained much interest due to their good characteristics, such as large surface area, good thermal stability, high uniformity, and controllable pore size [2]. There are many potential applications of silica nanostructures, such as adsorbents [3], drug delivery systems [4], and host of metal nanoparticles [5-6]. For the last example of applications, the silica nanomaterials have been used for growing of gold

nanoparticles (AuNPs) because they can help to control the size to give a uniform distribution of AuNPs [7]. Nowadays, AuNPs are one of the main research subjects in nanotechnology because of their unique properties for promising applications in electronic and optical devices; and biomedical fields, such as drug delivery vehicles and catalysts in many organic or inorganic reactions [8]. The unique properties of nanoparticles have been studied based on phenomenon of AuNPs with their electronic characteristics of surface plasmon resonance (SPR) band. Depending on the methods being used, AuNPs can be synthesized in a wide range of sizes or shapes, such as spheres, rods, flowers, cages, multi-branched and others. Since gold is the most stable element within its respective group, resilient to oxidation reactions and chemically inert, gold salts and their nanoparticles have been developed as catalysts in many chemical reactions. Generally, catalytic reaction using AuNPs can be performed either homogenously using colloidal gold solution or heterogeneously using gold nanocomposites. Interestingly, heterogeneous catalysis is more preferred compared to homogenous catalysis as it is much easier to recover the catalysts during the actual applications [9]. However, most of the reported heterogeneous catalysts were synthesized as powdered form that resulted in many limitations, such as high time consumption, loss of catalysts in recovery processes (filtration and centrifugation), catalyst contamination and low reusability with less than 10 cycles [10]. Considering catalysts in the powdered form can result in loss and contamination throughout the process, the thin film catalysts might also help to solve the problems.

While most common synthesis of thin film mainly uses glass as their main substrates, other reported works [11-12] also use anodized aluminium oxide (AAO) as their substrate during the film fabrication. Generally, AAO is comprised of ordered porous cylindrical channels having a vertical 1D arrangement. Generally, AAO can be either purchased commercially or synthesized in a lab-scale approach. AAO membrane can have pores sizes ranging from a few tens of nanometers to above one micron depending on the synthesis anodization parameters, including the voltage and the electrolyte acids [13]. AAO membrane is widely used and proven as a successful template for fabricating nanostructures, especially mesoporous materials due to its ordered large size pores. Furthermore, the pores can also be easily filled to produce samples with preferred orientations and dimensions, which can be applied for the usage of sensor, energy storage or electronic devices, and catalysis. For preparation as thin films, there are many techniques that can be utilized such as spin coating [14] and drop-casting [15]. The spin-coating technique can be divided into three main stages: deposition of the sample solution onto a flat substrate, spinning of the sample at desired rotation per minutes (rpm), and evaporation of the solvent. On the contrary, the drop-casting technique is done by simply dropping the sample directly onto the substrate before allowing the spontaneous solvent evaporation to occur. In brief, both fabrication techniques have their own advantages and disadvantages. In this work, thin film nanocomposites containing gold ions and silica sources were fabricated on different substrates (glass, AAO or both) using both spin-coating and drop-casting technique and their resulting properties were studied for potential application as heterogeneous catalyst containing AuNPs. The synthesis of AuNPs with a small size and sphere shape was done by utilizing thermal treatment at 210 °C under hydrogen environment as reported elsewhere [5]. It was expected that the fabrication of this nanocomposites as thin film will resolve the issue of low recovery and reusability at the end of the catalytic reaction.

II. MATERIALS AND METHODS

A. Materials

In this work, all the chemicals with analytical grade from Sigma-Aldrich brands were used. During the fabrication of thin film using the sol-gel solution, pipette from Thermofisher Scientific model Finnpipette F2 variable volume single-channel (10 to 100 μL) was used. The glass substrate used was a micro coverglass with 25 mm in sizes diameter while the AAO substrates used were commercially available Whatman Anodisc 25 mm in diameter.

B. Experiments and Characterisation

Gold(I) pyrazolate complex/silica ($[Au_3Pz_3]C_{10}$TEG/silica) film composite was firstly synthesized via sol-gel synthesis after the formation of columnar structures consisting of gold(I) pyrazolate complex as the template [16-18]. Firstly, a medium comprised of dry ethanol (61.6 mg, 1.25 mmol), deionized water (11.9 mg, 0.70 mmol) and hydrochloric acid (0.30 mg, 2.99×10^{-3} mmol) was prepared before being added to gold pyrazolate complex (10 mg, 2.49×10^{-3} mmol). The mixture was left to dissolve for 20 minutes before tetrabutoxysilane (TBOS, 48 mg, 1.49×10^{-1} mmol) was added into the solution. The sol-gel solution was covered in aluminium foil and aged for 12 hours at room temperature. The protocol was done as according to the ratio of $[Au_3Pz_3]C_{10}$TEG/ [TBOS]/ [EtOH]/ [HCl]/ [H_2O] = 1:60:504:10:1.2:266 to allow the partial oligomerization of TBOS to occur during the aging process. For fabrication as thin films, 70 μL of the final sol-gel solution can be either spin-coated or drop-casted on substrates such as glass to give $[Au_3Pz_3]C_{10}$TEG/silica_glass, on AAO to give $[Au_3Pz_3]C_{10}$TEG/silica_AAO, or both to give $[Au_3Pz_3]C_{10}$TEG/silica_AAO-glass. After the fabrication process, the thin films produced were left to dry in an enclosed container for 3 hours (ethanol vapour-mediated maturing) and additional 24 hours in open air. For synthesis of gold nanoparticles, the thermal hydrogen reduction under hydrogen gas was performed using Carbolite model STF 15/610 quartz tube furnace at 210 °C. The thermal hydrogen reduction was performed only to composite fabricate on the combination of both AAO-glass as it had the best quality of film. After the thermal hydrogen reduction, the Au(I) in the $[Au_3Pz_3]C_{10}$TEG/silica_AAO-glass was reduced to Au(0) to produce AuNPs/silica_AAO-glass film.

The presence of Au(I)-Au(I) interaction in the $[Au_3Pz_3]C_{10}$TEG/silica_AAO-glass was firstly confirmed by using fluorescent spectroscopy and its image was captured under hand-held ultraviolet light (254 nm). Moreover, the digital camera image of all films was also photographed under daylight while the in-depth surface analysis of the films was

studied by using light microscope image. Further structural analyses of thin films as well as the particles size of AuNPs were characterized using scanning electron microscope (SEM) and X-ray diffraction (XRD) analysis while the surface plasmon resonance of the AuNPs was studied using UV-vis spectroscopy. The sample morphology studied using scanning electron microscope was conducted on a Hitachi TM3000 (15 kV as the accelerating voltage) at 0.5 μm magnifications. The XRD analysis of the as-synthesized thin films was performed using Rigaku Smartlab X-ray diffractometer at scan rate of 0.02^{o} s^{-1} within the range of 1.5–60º. The absorption spectra for SPR phenomenon of the AuNPs were measured by using Shimadzu DR UV-Vis spectrophotometer (UV-2600) for solid samples. In addition, the AuNPs morphology and characterization were performed using transmission electron microscope model JEM-2100-TEM at 200 kV as operating voltage. For the TEM sample preparation, the AuNPs/silica composite that was fabricated inside AAO-glass needed to be immersed in 5 wt% of phosphoric acid (H_3PO_4) to dissolve the AAO template first before the sample was collected via filtration, dispersion and sonication in ethanol for 30 minutes. Later, a small amount of the well-dispersed sample was dropped onto a Lacey Formvar film copper grid, followed by an overnight drying before the TEM analysis. The surface roughness of AuNPs/silica_AAO-glass film was also studied and compared by using atomic force microscope (AFM) from JPK Instruments model NanoWizard 3 NanoScience equipped with Zeiss microscope (non-contact mode, resonant frequency 300 kHz, force constant 40 N m^{-1}).

III. RESULTS AND DISCUSSIONS

A. Development of Gold(I) Pyrazolate/Silica Composite Film ([Au$_3$Pz$_3$]C$_{10}$TEG/silica) on Various Substrates using Different Fabrication Techniques

In this stage, different coating techniques on several types of substrates were carried out to determine the best sample fabrication method that could produce the highest quality of thin film. Firstly, [Au_3Pz_3]C_{10}TEG/silica composite was synthesized via the sol-gel synthesis with one-dimensional arrangement in long-arrays of columnar assembly of gold(I) pyrazolate complex. A medium of aqueous acidic ethanolic was prepared before being added to gold complex. In this process, the gold complex acted as a template or structure-directing agent for the synthesis of silica composites. Later, TBOS that functioned as silica source was added into the solution. For fabrication as thin films, the final sol-gel solution was either spin-coated or drop-casted on several substrates, such as glass, anodized aluminium oxide (AAO) or combination of AAO-glass. For glass substrate, it was found that its hardness was beneficial to prevent the thin film samples from breaking easily. When the sol-gel solution was spin-coated at 3000 rpm for 15 seconds, a thin and uniform colourless film was successfully fabricated ([Au_3Pz_3]C_{10}TEG/silica_glass; Figure 1a). Although the resulting thin film [Au_3Pz_3]C_{10}TEG /silica_glass was stable enough to be characterized, the major problem with this fabrication technique was that a lot of samples was lost during the spinning stage, leaving only a small portion that coated the glass. Therefore, drop-casting method was also applied on glass substrate to form thin film [Au_3Pz_3]C_{10}TEG /silica_glass which resulted in a thick coating sample. The main advantage of drop-casting techniques is that sample loss can be completely prevented due to slowly dropping onto the substrate, resulting in a higher amount of coated sample. Unfortunately, it was found that the thick coating only made the fabricated nanocomposite to crack and be easily peeled off from the glass substrate, hence making it difficult to carry out any characterizations on the film (Figure 1b).

Moreover, for fabrication of thin film by using AAO substrate, only drop-casting approach was suitable to be applied as AAO was very brittle and easy to break. The sol-gel solution was carefully drop-casted on AAO substrate to successfully produce thin film [Au_3Pz_3]C_{10}TEG/silica_AAO. Interestingly, it was observed that the nanocomposite coated on AAO did not show any cracks (Figure 1c). This might indicate that the infiltration of the sol-gel inside the porous structure of AAO resulted in a higher stability of thin film sample. However, as the commercial AAO substrates did not have a bottom part [19], some portion of the drop-casted nanocomposites leaked out from the AAO bottom. Furthermore, the brittleness of AAO substrate also limited the characterization or practical usage of the films. As a result, a thin film system that utilized the combination of both substrates was developed to solve the weakness of individual glass or AAO substrate via drop-casting fabrication method. In this case, the hardness of glass can be exploited to support the brittleness of AAO substrate. In addition, the nanocomposite in the form of sol-gel solution was also acted as an adhesive to physically bind both substrates together after the drop-casting step to form film [Au_3Pz_3]C_{10}TEG/silica_AAO-glass with greyish brown colour (Figure 1d). The AAO substrate was placed at the top to receive and confine the resulting gold/ silica composite in its pore while glass substrate was placed at the bottom to prevent the sol-gel solution from leaking out from the AAO pore. All the comparison for different fabrication techniques on various substrates mentioned earlier was summarized in Table I while their photography images were shown in Figure 1. Further characterization was only done to film fabrication on AAO-glass as it showed the highest quality and stability.

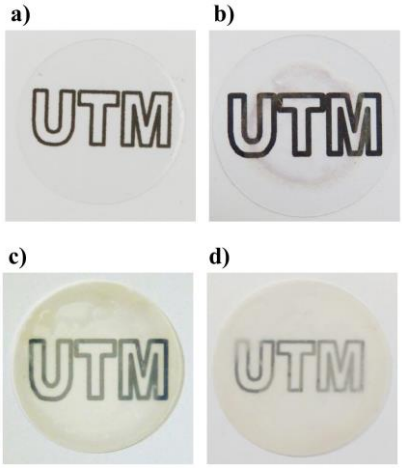

Fig. 1 The photography images under daylight for [Au_3Pz_3]C_{10}TEG/silica film on a) glass only after spin-coating, b) glass only after drop-casting, c) AAO only after drop-casting, and d) AAO-glass after drop-casting showing all films were quite transparent even when being placed against a Universiti Teknologi Malaysia (UTM) background.

TABLE I. THE COMPARISON OF DIFFERENT FABRICATION TECHNIQUES ON VARIOUS SUBSTRATES FOR SYNTHESIS OF GOLD(I) PYRAZOLATE/SILICA ($[AU_3PZ_3]C_{10}$TEG /SILICA) FILMS

Substrates	Fabrication Techniques	Advantages	Disadvantages
Glass	Spin-coating 3000 rpm	• Thin and uniform coating • Glass substrate was hard and did not easily break during handling • Convenient for characterizations	• Loss of sample during spinning to give low amount of composites coated on substrate
Glass	Drop-casting	• Higher amount of nanocomposite was coated • Glass substrate was hard and did not easily break during handling	• Thick and poor uniformity on film • The thick nanocomposites cracks and peeled off • Difficult for characterizations
AAO	Drop-casting	• Higher amount of nanocomposite was coated	• The AAO substrate was very brittle and easy to break • The drop-casted composites leaked out from the AAO bottom • Difficult for characterizations
AAO-glass	Drop-casting	• Higher amount of nanocomposites was coated • The hard glass will support the brittleness of AAO substrate • Convenient for characterizations	• Thick coating

B. Characterization of Gold(I) Pyrazolate/Silica ([Au₃Pz₃]C₁₀TEG/silica) and Gold Nanoparticles/ Silica (AuNPs/silica) Composite Film on Anodized Aluminium Oxide-Glass Substrate

Figure 2a and 2b showed the photograph images of empty AAO substrate and $[Au_3Pz_3]C_{10}$TEG/silica_AAO-glass under hand-held UV lamp 254 nm. The empty AAO substrate only reflected the UV light 254 nm under dark condition to give a blue visualization (Figure 2a). In contrast, $[Au_3Pz_3]C_{10}$TEG/silica_AAO-glass film showed a pinkish red color under UV light, suggesting the preservation of Au(I)-Au(I) interactions even after its fabrication as thin films (Figure 2b).

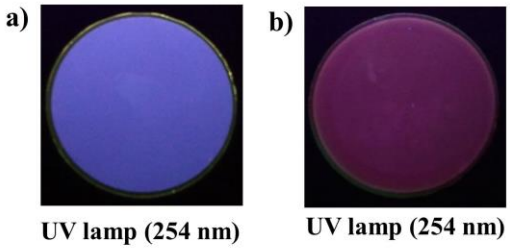

Fig. 2 The photography images under hand-held UV lamp 254 nm of a) empty AAO substrate and b) $[Au_3Pz_3]C_{10}$TEG/silica_AAO-glass

In addition, the luminescent spectrum of thin film $[Au_3Pz_3]C_{10}$TEG/silica_AAO-glass was observed at 692 nm upon excitation at 276 nm with Stokes shift of 416 nm (Figure 3). This result was in good agreement with the pinkish-red colour of the thin film under UV light 254 nm to prove the preservation of aurophilic interaction in the composite film.

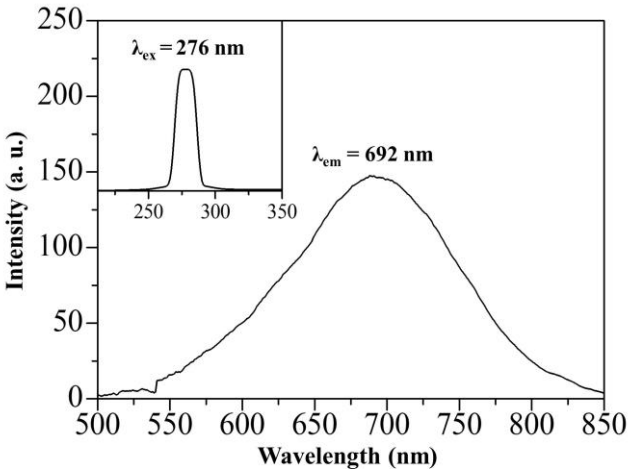

Fig. 3. Emission spectrum of $[Au_3Pz_3]C_{10}$TEG/silica_AAO-glass (λ_{em} = 692 nm) with inset figure showing the excitation spectrum (λ_{ex} = 276 nm) having Stokes shift of 416 nm

For the structural analysis of the resulting $[Au_3Pz_3]C_{10}$TEG/silica_AAO-glass and AuNPs/silica_AAO-glass (after thermal hydrogen reduction at 210 °C for 2 hours), XRD measurement at small-angle and wide-angle region was conducted as presented in Figure 4. Although there were no apparent peaks being observed at small-angle region for both $[Au_3Pz_3]C_{10}$TEG/silica_AAO-glass (blue line) and AuNPs/silica_AAO-glass (black line), the presence of AuNPs

after heat treatment was confirmed in AuNPs/silica_AAO-glass film with diffraction peak at 2θ = 38.20º for d_{111} plane having average size of 13.9 nm based on the calculation using Scherrer's equation. The absence of any distinct peaks at small-angle region suggested that the sol-gel sample after being drop-casted was grown perpendicularly to the glass substrate and in parallel according to the 1D direction of AAO pores [20].

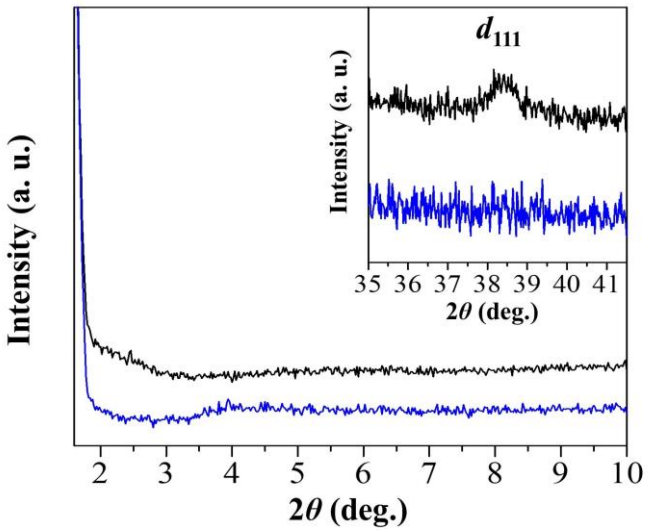

Fig. 4: a) XRD peak at small-angle region of $[Au_3Pz_3]C_{10}$TEG/silica_AAO-glass (blue line) and AuNPs/silica_AAO-glass (black line) with inset figure of XRD peak at wide-angle region indicating the presence of AuNPs having d_{111} lattice

Interestingly, the successful formation of AuNPs was further supported by the SPR study of AuNPs/silica_AAO-glass film with absorption peak at 545 nm (Figure 5) accompanied with the change of light-brownish color of $[Au_3Pz_3]C_{10}$TEG/silica_AAO-glass (Figure 1d) to deep-red AuNPs/silica_AAO-glass film in daylight (inset Figure 5).

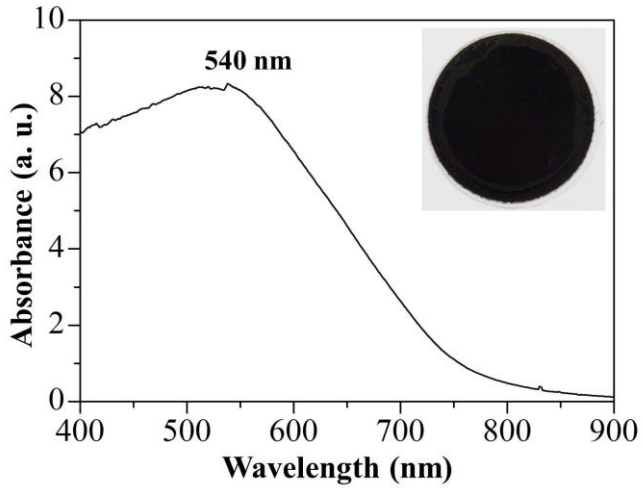

Fig. 5. Absorption spectrum of AuNPs/silica_AAO-glass for SPR study of AuNPs with inset figure of deep-red AuNPs/silica_AAO-glass at daylight

Further characterizations in comparison with empty AAO substrate using light microscopy, SEM, AFM dan TEM were also conducted on AuNPs/silica_AAO-glass film as this film was the intended sample for any future applications. Figure 6a and 6c show the light microscope and SEM images of empty AAO substrate while Figure 6b and 6d show the light microscope and SEM images of AuNPs/silica_AAO-glass film. When compared to empty AAO substrate, the deep-red AuNPs/silica_AAO-glass film in Figure 6b showed a smooth and uniform surface without visible cracks, implying the successful fabrication of sol-gel solution onto the AAO substrate. SEM analysis that was carried out for analysing the film surface at a higher magnification also showed the successful filling of most AAO pores within 100 to 200 nm in diameter with AuNPs/silica composite (Figure 6d). The presence of AuNPs is not visible in Figure 6d probably due to its small size and successful fabrication inside the AAO pores.

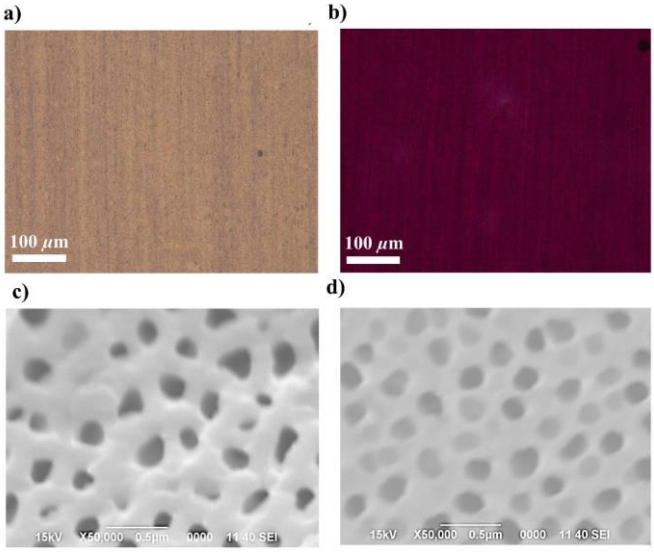

Fig. 6. Light microscopy images of a) empty AAO substrate, b) AuNPs/silica_AAO-glass at magnification scale of 100 μm and their corresponding SEM images of c) empty AAO substrate and d) AuNPs/silica_AAO-glass at magnification scale of 0.5 μm with accelerating voltage of 15 kV

The AFM study in Figure 7 was mainly done to investigate the surface roughness of the empty AAO substrate and AuNPs/silica_AAO-glass film after the sol-gel process (drop-casting onto the substrates) followed by heat treatment as the final assemblies would result in a certain degree of roughness and compactness. Based on the 2D and 3D representation of empty AAO substrate (Figure 7a and 7b), the empty channels of AAO could be clearly observed throughout the whole image with its surface roughness calculated to be 64.38 nm. On the other hand, after the fabrication of AuNPs/silica_AAO-glass film, the surface roughness was decreased to 18.81 nm, indicating the empty pores of AAO being filled in to produce a smoother surface on the film (Figure 7c and 7d).

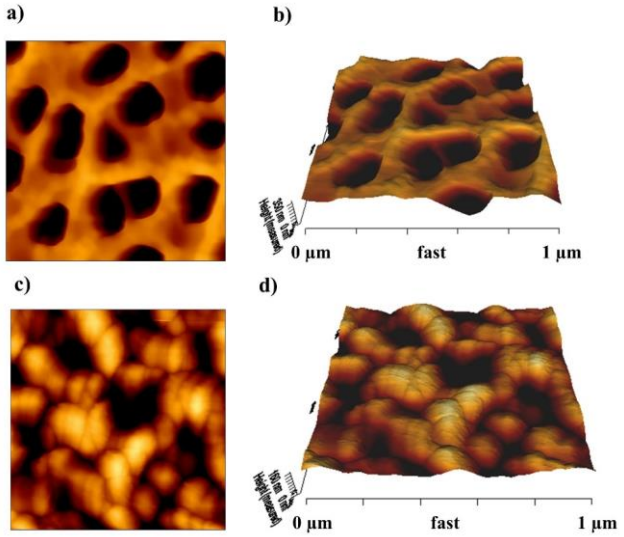

Fig. 7. The 1 µm X 1 µm AFM images of empty AAO substrate at a) 2D and b) 3D images as well as AuNPs/silica_AAO-glass at c) 2D and d) 3D images

Moreover, TEM analysis also was carried out to study the morphology of the resulting AuNPs/silica_AAO-glass film. In this case, the AAO must be removed first by immersing the film in 5 wt% of phosphoric acid while the glass substrate was taken away during the filtration process to collect the remaining sample. The TEM image in Figure 8a clearly shows the formation of silica nanorod containing many spherical AuNPs. The diameter of the mesoporous silica nanorod was measured to be 150 nm and in good agreement with size of AAO pores while the particle size of AuNPs was between 5 to 25 nm as according to the image. In Figure 8b, AuNPs with a fringe spacing of 0.23 nm was observed with corresponding to 111 plane (d_{111}) of *face centered cubic* (*fcc*) based on FFT pattern (top inset figure) and auto-correlation image (bottom inset figure) at 2θ = 38.20º (JCPDS no.04-0784) as supported by the XRD spectrum in inset Figure 4.

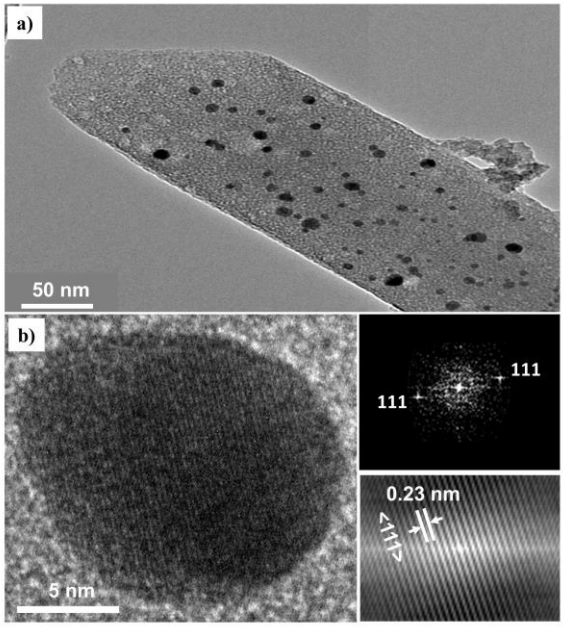

Fig. 8**:** TEM images of **AuNPs/silica_AAO-glass** showed a successful formation of a) spherical AuNPs in the silica matrix after the removal of AAO template via acid treatment at 50 nm scale bar, b) AuNPs having d_{111} lattice with its corresponding FFT pattern (top inset figure) and auto-correlation image (bottom inset figure).

By using energy-dispersive X-ray (EDX) elemental analysis, the possible elemental composition and purity of the as-synthesized AuNPs/silica_AAO-glass film was evaluated. Based on Figure 9, two distinctive peaks around 2.0 keV due to Si and Au as significant elements were observed, confirming the formation of AuNPs in the silica matrix. Another sharp peak for O appeared around 0.5 keV while the other small bands corresponding to C and Cu appeared probably due to the use of Lacey Formvar film copper grid while the sample preparation for TEM analysis was carried out. The smaller weight percentage of Au (7.52%) compared to Si (31.21%) shown in Table II was relatively significant with the mol ratio used during the sol-gel synthesis between gold source ($[Au_3Pz_3]C_{10}$TEG) and silica source (TBOS) where silica source was added abundantly to act as silica matrix to grow AuNPs while embedded inside AAO.

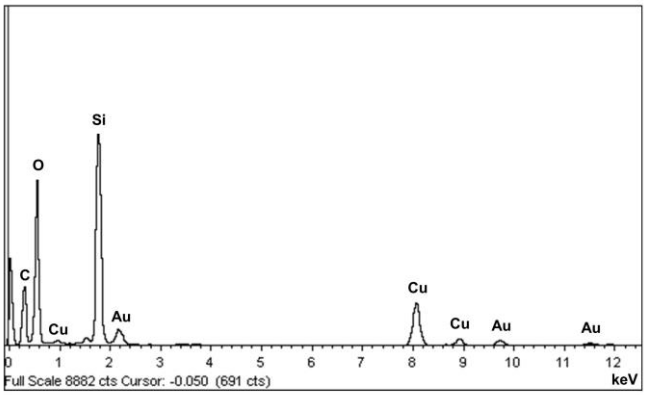

Fig. 9. EDX of TEM images of AuNPs/silica_AAO-glass film after the removal of AAO template via acid treatment

TABLE II. THE ELEMENTAL COMPOSITION IN AuNPs/SILICA_AAO-GLASS FILM BASED ON THE EDX ANALYSIS

Element	Weight%	Atomic%
C	12.83	23.46
O	33.66	46.20
Si	31.21	24.40
Cu	14.78	5.11
Au	7.52	0.84
Totals	100.00	

IV. CONCLUSIONS

This work firstly focused on the fabrication of $[Au_3Pz_3]C_{10}$TEG/silica thin film on either glass, anodized alumina oxide (AAO) or both using spin-coating or drop-casting technique. It was found that $[Au_3Pz_3]C_{10}$TEG/silica fabricated on combination of both AAO-glass substrate gave the best quality based on its surface thickness, layer uniformity and film brittleness. Moreover, preservation of Au(I)-Au(I) interaction in $[Au_3Pz_3]C_{10}$TEG/silica_AAO-glass thin film was shown based on its luminescent spectrum at 692 nm upon excitation at 276 nm (Stokes shift: 416 nm) and its

pinkish-red colour under UV light (254 nm). Later, AuNPs/silica_AAO-glass film was produced after the $[Au_3Pz_3]C_{10}$TEG/silica_AAO-glass was subjected to thermal hydrogen reduction at 210 °C for 2 hours. The successful synthesis of AuNPs in the film was confirmed based on the deep-red colour of AuNPs/silica_AAO-glass film, SPR peak at 545 nm, XRD pattern at $2\theta = 38.20^{o}$ corresponding to d_{111} plane in wide-angle region, and spherical shapes found in TEM images with small particle size between 5 to 25 nm. SEM and AFM images also indicated a uniform and high quality of fabricated AuNPs/silica_AAO-glass film that was suitable for further applications. Future works include the application of the resulting AuNPs/silica_AAO-glass film as a potential heterogeneous catalyst in degradation of hazardous compounds or dyes commonly found in wastewater. Considering catalysts in the powdered form can result in loss, low reusability and contamination throughout the process, this thin film catalysts might potentially help to resolve the issue.

CONFLICT OF INTEREST

The authors declare that there is no conflict of interest regarding the publication of this paper.

ACKNOWLEDGEMENT

The authors are grateful to Fundamental Research Grant Scheme (FGRS) from Ministry of Higher Education (MOHE) of Malaysia under vote FRGS/1/2020/STG05/USIM/03/2 (P5-2-50-52120-KPT-FRGS-KGI) for financial support. The authors also thank Centre for Sustainable Nanomaterials, Ibnu Sina Institute for Scientific and Industrial Research (ISI-SIR), Universiti Teknologi Malaysia (UTM), Malaysia as well as Universiti Sains Islam Malaysia (USIM) for characterization facilities.

REFERENCES

[1] Camargo, P. H. C., Satyanarayana, K. G. and Wypych, F. (2009). Nanocomposites: Synthesis, structure, properties and new application opportunities. *Materials Research, 12(1),* 1-39. https://doi.org/10.1590/S1516-14392009000100002

[2] Kankala, R.K., Han, Y.H., Na, J., Lee, C.H., Sun, Z., Wang, S.B., Kimura, T., Ok, Y.S., Yamauchi, Y., Chen, A.Z. and Wu, K.C.W., (2020). Nanoarchitectured structure and surface biofunctionality of mesoporous silica nanoparticles. *Advanced materials*, *32*(23), p.1907035. https://doi.org/10.1002/adma.201907035

[3] Mirbagheri, R., Elhamifar, D., & Shaker, M. (2021). Yolk–shell structured magnetic mesoporous silica: A novel and highly efficient adsorbent for removal of methylene blue. *Scientific Reports*, 11(1), 23259. https://doi.org/10.1038/s41598-021-02699-w

[4] Dumontel, B., Conejo-Rodríguez, V., Vallet-Regí, M., & Manzano, M. (2023). Natural Biopolymers as Smart Coating Materials of Mesoporous Silica Nanoparticles for Drug Delivery. *Pharmaceutics*, 15(2), 447. https://doi.org/10.3390/pharmaceutics15020447

[5] Jalani, M. A., Yuliati, L., Lee, S. L., & Lintang, H. O. (2019). Highly ordered mesoporous silica film nanocomposites containing gold nanoparticles for the catalytic reduction of 4-nitrophenol. *Beilstein Journal of Nanotechnology*, *10(1),* 1368-1379. https://doi.org/10.3762/bjnano.10.135

[6] Mulikova, T., Abduraimova, A., Molkenova, A., Em, S., Duisenbayeva, B., Han, D. W. and Atabaev, T. S. (2021). Mesoporous silica decorated with gold nanoparticles as a promising nanoprobe for effective CT X-ray attenuation and potential drug delivery. *Nano-Structures & Nano-Objects*, *26*, 1-5. https://doi.org/10.1016/j.nanoso.2021.100712

[7] Pourhassan, F., Khalifeh, R. and Eshghi, H. (2021). Well dispersed gold nanoparticles into the multi amine functionalized SBA-15 for green chemical fixation of carbon dioxide to cyclic carbonates under solvent free conditions. *Fuel*, *287*, 1-12. https://doi.org/10.1016/j.fuel.2020.119567

[8] Witzel, S., Hashmi, A. S. K., & Xie, J. (2021). Light in gold catalysis. *Chemical Reviews*, 121(14), 8868-8925. https://doi.org/10.1021/acs.chemrev.0c00841

[9] Swathi, R. S. and Sebastian, K. L. (2008). Molecular mechanism of heterogeneous catalysis. *Resonance*, *13(6),* 548-560. https://doi.org/10.1007/s12045-008-0061-6

[10] Shokouhimehr, M. (2015). Magnetically separable and sustainable nanostructured catalysts for heterogeneous reduction of nitroaromatics. *Catalysts*, *5(2)*, 534-560. https://doi.org/10.3390/catal5020534

[11] Lintang, H. O., Jalani, M. A., Yuliati, L., & Salleh, M. M. (2017, May). Fabrication of mesoporous silica/alumina hybrid membrane film nanocomposites using template sol-gel synthesis of amphiphilic triphenylene. In *IOP Conference Series: Materials Science and Engineering* (Vol. 202, No. 1, p. 012003). IOP Publishing. https://doi.org/10.1088/1757-899X/202/1/012003

[12] Yazid, H., Hadzir, N. M., Adnan, R., & Jani, A. M. M. (2022). Gold decorated on anodic aluminium oxide and its unique catalytic activity. *Materials Today: Proceedings*, 66, 4000-4004. https://doi.org/10.1016/j.matpr.2022.04.94

[13] Zhang, J., Kielbasa, J. E. and Carroll, D. L. (2010). Controllable fabrication of porous alumina templates for nanostructures synthesis. *Materials Chemistry and Physics*, *122(1),* 295-300. https://doi.org/10.1016/j.matchemphys.2010.02.023

[14] Barzinjy, A. A., Hamad, S. M., Esmaeel, M. M., Aydın, S. K., & Hussain, F. H. S. (2020). Biosynthesis and characterisation of zinc oxide nanoparticles from Punica granatum (pomegranate) juice extract and its application in thin films preparation by spin-coating method. *Micro & Nano Letters*, 15(6), 415-420. https://doi.org/10.1049/mnl.2019.0501

[15] Shrestha, N. K., Patil, S. A., Cho, S., Jo, Y., Kim, H., & Im, H. (2020). Cu–Fe–NH_2 based metal–organic framework nanosheets via drop-casting for highly efficient oxygen evolution catalysts durable at ultrahigh currents. *Journal of Materials Chemistry A*, 8(46), 24408-24418. DOI https://doi.org/10.1039/D0TA07716J

[16] Jalani, M. A., Yuliati, L., Lee, S. L., & Lintang, H. O. (2018). Size-exclusion liquid chromatography for effective purification of amphiphilic trinuclear gold(I) pyrazolate complex. *Malaysian Journal of Fundamental and Applied Sciences*, *14*, 133-137. https://doi.org/10.11113/mjfas.v14n1-2.953

[17] Jalani, M. A. A. K., Lintang, H. O., Lee, S. L., Matmin, J., Ghazalli, N. F., Yuliati, L., Ajid A. Z. and Idrus, M.I. (2021). Temperature-Dependent X-Ray Studies of Discotic Hexagonal Columnar Mesophases in Trinuclear Gold (I) Pyrazolate Complex. *Malaysian Journal of Fundamental and Applied Sciences*, *17*, 285-294. https://doi.org/10.11113/mjfas.v17n3.2112

[18] Lintang, H. O., Kinbara, K., Tanaka, K., Yamashita, T. and Aida, T. (2010a). Self-repair of a one-dimensional molecular assembly in mesoporous silica by a nanoscopic template effect. *Angewandte Chemie International Edition*, *49(25),* 4241-4245. https://doi.org/10.1002/ange.200906578

[19] Koblischka, M. R., Zeng, X. L. and Hartmann, U. (2016). Commercial alumina templates as base to fabricate 123-type high-T_C superconductor nanowires. *Physica Status Solidi (a)*, *213(4)*, 1069-1076. https://doi.org/10.1002/pssa.201532475

[20] Hillhouse, H. W., Van Egmond, J. W., Tsapatsis, M., Hanson, J. C. and Larese, J. Z (2001). The interpretation of x-ray diffraction data for the determination of channel orientation in mesoporous films. *Microporous and Mesoporous Materials*, *44*, 639-64. https://doi.org/10.1016/S1387-1811(01)00244-X